

Twin Boundary Defect Structure in Bismuth Telluride

D.L. Medlin and N.Y.C. Yang

Sandia National Laboratories, 7011 East Avenue, Livermore CA 94551

Bismuth telluride and its alloys are widely used for thermoelectric energy conversion for applications in both solid-state cooling and power generation. Control of grain structure is an important aspect of engineering Bi_2Te_3 -based thermoelectric materials[1]. Optimizing the grain alignment, or crystal texture, can improve the thermoelectric performance of polycrystalline Bi_2Te_3 -based materials because of their anisotropic single-crystal transport properties. Furthermore, by reducing the grain size to nanoscale dimensions, enhancements to thermoelectric performance can be obtained through reduced thermal conductivity due to phonon-scattering at the high density of embedded interfaces. At present, however, little is known concerning the atomic structure of grain boundaries in this material. In this presentation, I will discuss our recent electron microscopic studies of grain boundary structure in Bi_2Te_3 , focusing on defects present at the (0001) basal twin.

Within a single crystal of Bi_2Te_3 , the stacking of basal planes can be written as:

$$\dots \text{A}\beta\text{C}\alpha\text{B C}\alpha\text{B}\gamma\text{A B}\gamma\text{A}\beta\text{C} \dots \quad (1)$$

Here, the Te positions are indicated by Roman letters and the Bi position by Greek letters, so that a single 5-layer, $\dots : \text{Te}^{(1)}\text{-Bi-Te}^{(2)}\text{-Bi-Te}^{(1)} : \dots$, quintet of the Bi_2Te_3 structure is given by a unit such as $\text{A}\beta\text{C}\alpha\text{B}$ (a full unit cell of Bi_2Te_3 consists of three 5-layer packets). At a (0001) basal twin, the two adjacent crystals are related to each other by a 180° degree rotation about the c-axis. Electron microscopic observations and density functional theory calculations have shown that the structure of the Bi_2Te_3 basal twin consists simply of a reversal of the basal plane stacking sequence and that this reversal occurs at the $\text{Te}^{(1)}$ type planes (as indicated below by the underscore) [2]:

$$\dots \text{A}\beta\text{C}\alpha\text{B C}\alpha\text{B}\gamma\text{A} \text{C}\beta\text{A}\gamma\text{B} \dots, \quad (2)$$

In this presentation, we move beyond the simple structure of an ideal (0001) twin by considering the introduction of defects to this interface. We investigate the dislocation content of step-defects at a (0001) Bi_2Te_3 basal twin, an example of which is shown in Fig. 1. We then discuss more generally the defect crystallography for twins in Bi_2Te_3 by analyzing the dislocation content and step geometry for differently terminated step arrangements and comparing the relevant defect arrangements anticipated for deformation and annealing/growth twins (Fig. 2). Finally, we consider the observed defect in the context of this framework and discuss its relationship to analogous features observed in face-centered-cubic (FCC) metals, namely the $\{112\}$ -type interfaces that are commonly observed terminating $\{111\}$ growth and annealing twins in these materials.

References

- [1] D.L. Medlin and G.J. Snyder, *Current Opinion in Colloid and Interface Science* 14 (2009) 226.
- [2] D.L. Medlin, Q.M. Ramasse, C.D. Spataru, N.Y.C. Yang, *J. of Appl. Phys.* 108 (2010) 043517.
- [3] D.L. Medlin and N.Y.C. Yang, *J. Elect. Mat.*, in press (2012) doi: 10.1007/s11664-011-1859-7.
- [4] Sandia National Laboratories is a multi-program laboratory managed and operated by Sandia Corporation, a wholly owned subsidiary of Lockheed Martin Corporation, for the U.S. Department of Energy's National Nuclear Security Administration under contract DE-AC04-94AL85000. Support for this project was provided in part by the Sandia LDRD office.

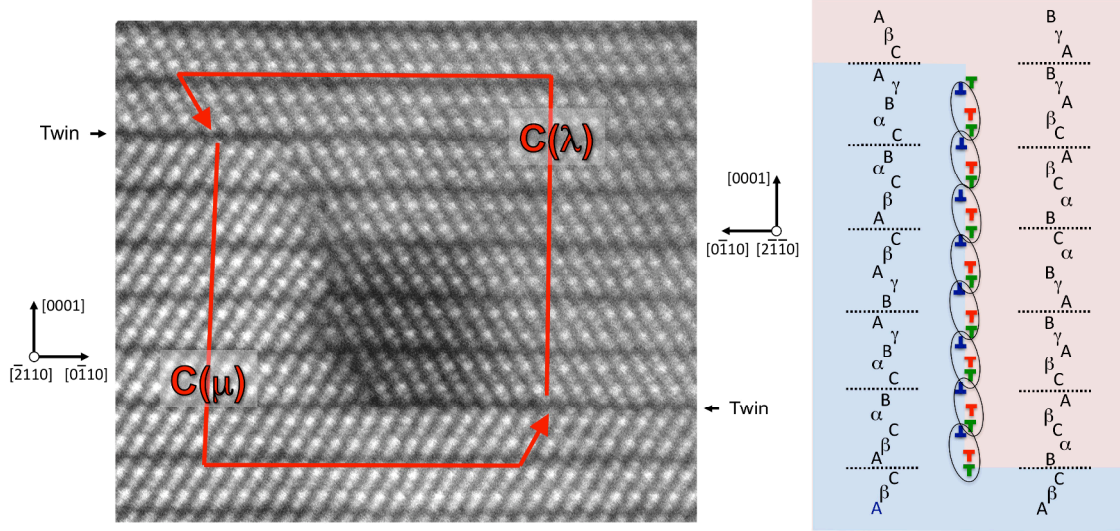


FIG. 1. (a) STEM-HAADF image of twin boundary step in Bi_2Te_3 . The (0001) twin interfaces on either side of the step are terminated at $\text{Te}^{(1)}$ -type planes. The white arrows indicate the circuit paths used to determine the Burgers vector of the step. Here, $C(\lambda) = 52 \times \frac{1}{6}[0\bar{1}10] + \frac{5}{3}[0001]$ and $PC(\mu) = 53 \times \frac{1}{6}[01\bar{1}0] + \frac{5}{3}[000\bar{1}] \pm \frac{1}{6}[2\bar{1}\bar{1}0]$, where P converts vectors from the lower crystal coordinates to those of the upper crystal. The resulting Burgers vector for the step, expressed in the coordinates of the upper crystal, is $\mathbf{b} = \frac{1}{3}[1\bar{1}00]$ or $\frac{1}{3}[\bar{1}010]$. Schematic on left shows one possible arrangement of $\frac{1}{3}<01\bar{1}0>$ -type twinning dislocations. These are distributed equally amongst the three possible orientations such that the net Burgers vector will cancel every three planes allowing the steps to cluster together and thereby avoid extended segments of unfavorably terminated (0001) twin.

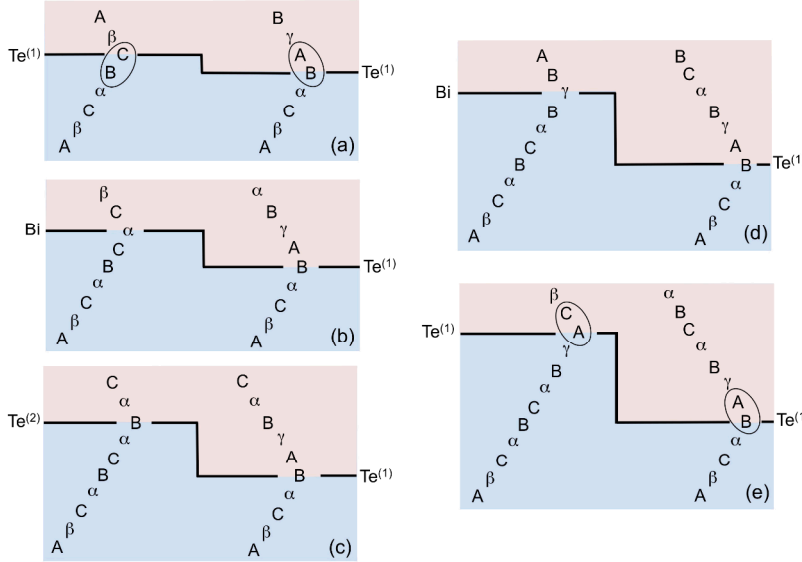


FIG. 2. Comparison of twin step configurations for step heights of $h=1$ through 5. Stacking of the (0001) planes is indicated by lettering with Greek letters for Bi planes and Roman letters for Te planes. The configurations shown in (a) $h=1$ $\text{Te}^{(1)}/\text{Te}^{(1)}$ and (b) $h=5$ $\text{Te}^{(1)}/\text{Te}^{(1)}$ terminate at equivalent, low-energy twin planes on either side of the step. The configuration in (a) is inverted on the two sides of the defect, with the double Te layer below the twin at the left and above the twin on the right. In (e) the configurations the double Te layer is above the twin on both sides and the structure is not inverted. The remainder of the configurations shown here terminate at crystallographically inequivalent sites.